https://doi.org/10.2352/EI.2023.35.14.COIMG-157

Plug-and-Play Sparse X-ray Phase Contrast Dark Field Tomography

Johnathan Mulcahy-Stanislawczyk, Amber L. Dagel; Sandia National Laboratories; Albuquerque, New Mexico, USA

Abstract

X-Ray phase contrast imaging (XPCI) augments absorption radiography with additional information related to the refractive and scattering properties of a sample. Grating-based XPCI allows broadband laboratory x-ray sources to be used, increasing the technique's accessibility. However, grating-based techniques require repeatedly moving a grating and capturing an image at each location. Additionally, the gratings themselves are absorptive, reducing x-ray flux. As a result, data acquisition times and radiation dosages present a hurdle to practical application of XPCI tomography.

We present a plug-and-play (PnP) reconstruction method for XPCI dark field tomographic reconstruction with sparse views. Dark field XPCI radiographs contain information about a sample's microstructure and scatter. The dark field reveals subpixel sample properties, including crystalline structure and material interfaces. This makes dark field images differently distributed from traditional absorption radiographs and natural imagery. PnP methods give greater control over reconstruction regularization compared to traditional iterative reconstruction techniques, which is especially useful given the dark field's unique distribution. PnP allows us to collect dark field tomographic datasets with fewer projections, increasing XPCI's practicality by reducing the amount of data needed for 3D reconstruction.

Introduction

X-Ray Phase Contrast Imaging (XPCI) in combination with computed tomography (CT) allows 3D reconstruction of an object's absorptive, refractive and scattering properties. This additional information beyond traditional absorption x-ray CT aids in material identification by improving contrast in low density materials, highlighting material boundaries and providing insight into material microstructure. XPCI utilizing gratings in a Talbot-Lau interferometer allows this technique to be used with a broadband, large focal spot lab-based x-ray tube rather than requiring a highly coherent source such as a costly and scarce synchrotron.

However, while the use of gratings makes XPCI more accessible via reduced source coherence requirements, it can significantly increase acquisition time of a radiographic or tomographic dataset. This is because gratings-based XPCI radiography requires stepping or translating one of the gratings and acquiring an image at each of those grating positions. It's common for a single XPCI radiograph to require a minimum of four or potentially more than 20 images taken with different grating positions. Collecting full CT datasets with many views can take hours or days.

Sparse view reconstruction could reduce this data requirement; however, most techniques depend upon specifying some regularizing assumptions about the distribution of reconstructed images. Under a Bayesian interpretation of this problem, those assumptions correspond to a prior model. As seen in Figure 1, the distribution of the scattering or dark field can be very different than traditional radiographs or natural imagery. Figure 1 appears almost edge detected, which is a stressing case for image assumption models like total variation. Sparse view dark field tomographic reconstruction therefore will benefit from incorporating an advanced prior model that can suppress reconstruction artifacts while retaining true sample signal.

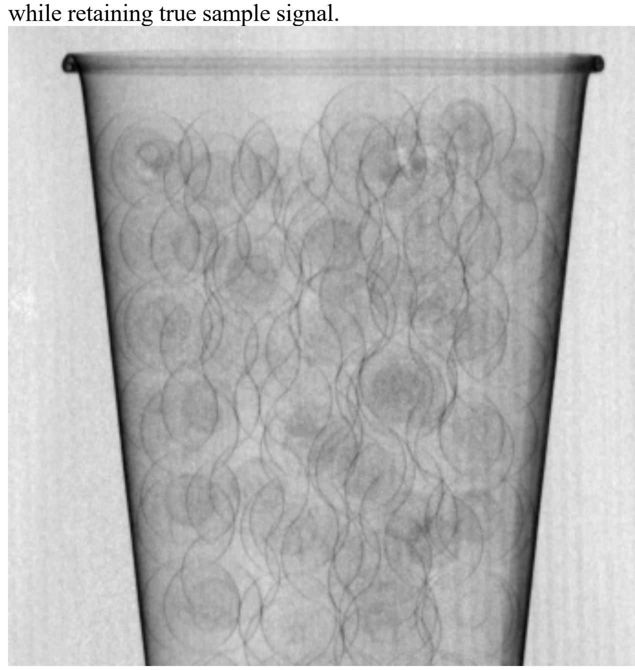

Figure 1: Example dark field image of wax paper cup filled with plastic spheres. The sample appears nearly edge detected, which is poor match for regularization techniques such as total variation.

We demonstrate a method for dark field CT with sparse views utilizing the plug-and-play prior (PnP) framework. This framework enables us to utilize advanced image priors that produce good reconstructions even on data that is nearly edge detected. We show that this technique outperforms tomographic reconstruction in both the unregularized least squares and total variation regularized cases.

Method

Our reconstruction method is based upon the PnP framework [1, 2]. Briefly, PnP generalizes this optimization objective seen in many inverse problems.

$$\underset{x}{\operatorname{argmin}} \|y - Ax\|^2 + \lambda R(x) \tag{1}$$

Here x is the desired reconstructed volume, y is the measured projections at various angles around the sample and A is the radon transform. The first term in the objective then drives the reconstruction toward matching the measured data and the imaging model. The second term $R(x)$ is a regularization function, which

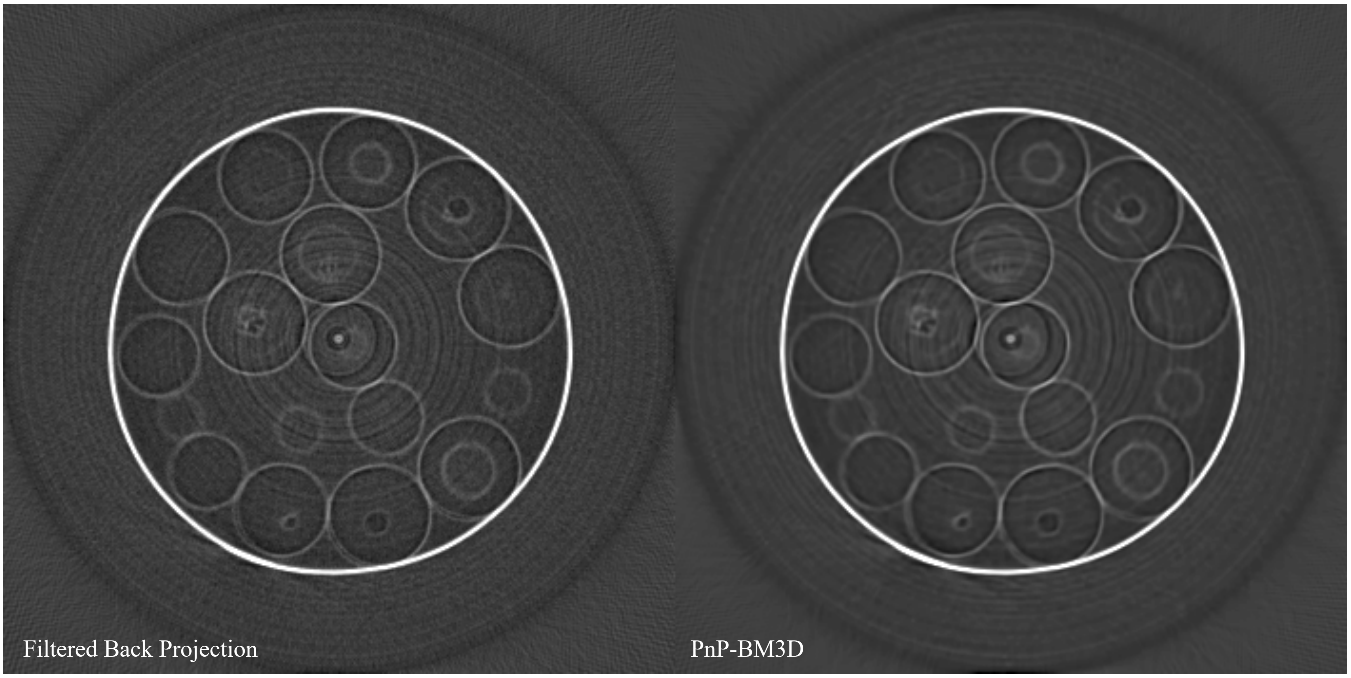

Figure 2: Unregularized least squares (left) and BM3D regularized (right) reconstructions with 450 views. Even in this well sampled case, the BM3D regularization removes some noise and ring artifacts while leaving the sample signal intact.

under a Bayesian interpretation corresponds to a prior model on the distribution of a reconstructed image in a maximum a posteriori estimate. Regularization is needed to reduce reconstruction artifacts due to any combination of undersampling, noise in the measurements, modeling error and more. The parameter λ controls how much the optimization favors matching the data model versus the regularization model.

PnP replaces that optimization objective with the concept of finding an equilibrium or fixed point between two or more models. The models are represented by some function or agent that pushes a given solution toward an assumption, such as data fidelity or regularity. Besides this convenient structure, PnP allows advanced regularization models in the form of image denoisers to be used. From a loose Bayesian perspective, these image denoisers can be thought of as containing an implicit prior model. The key to their utility is not that they specifically remove noise or imaging artifacts but that they remove data inconsistent with their implicit model of how images should be distributed.

For the data model with $\tilde{x}$ representing a current estimate of the 3D volume, PnP requires solving this optimization problem:

$$\underset{x}{\operatorname{argmin}} \|y - Ax\|^2 + \lambda \|x - \tilde{x}\|^2 \quad (2)$$

We solve this utilizing LSMR [3] from Krylov.jl [4]. For the prior models, we show results utilizing total variation and block matching 3D (BM3D) [5].

Results

We reconstructed a 3D slice of the volume corresponding to the sample in Figure 1 with 450 views and 90 views collected uniformly around 360 degrees of the sample. The projections are additionally negative log transformed to comply with Beer's law for exponential signal extinction. Figure 2 shows reconstructions with 450 views.

Qualitatively, the results are similar because the dataset is well sampled. The BM3D regularization has some small reduction of noise and ring artifacts.

Figure 2 shows reconstructions with several techniques with 90 views. The filtered back projection and unregularized least squares reconstructions have significant radial aliasing artifacts and salt and pepper noise. Total variation has less noise and artifacts, but the regularization blurs the sample, resulting in less contrast. The BM3D regularized reconstruction has some artifacts but leaves the sample very sharp.

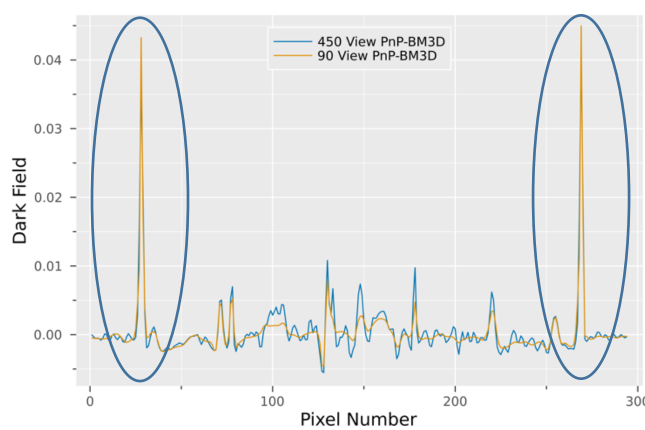

Figure 3: Pixel values along the middle row of the 450 and 90 view BM3D reconstructions seen across Figure 2 and Figure 4. The 90 view case shows good correspondence to the 450 view case.

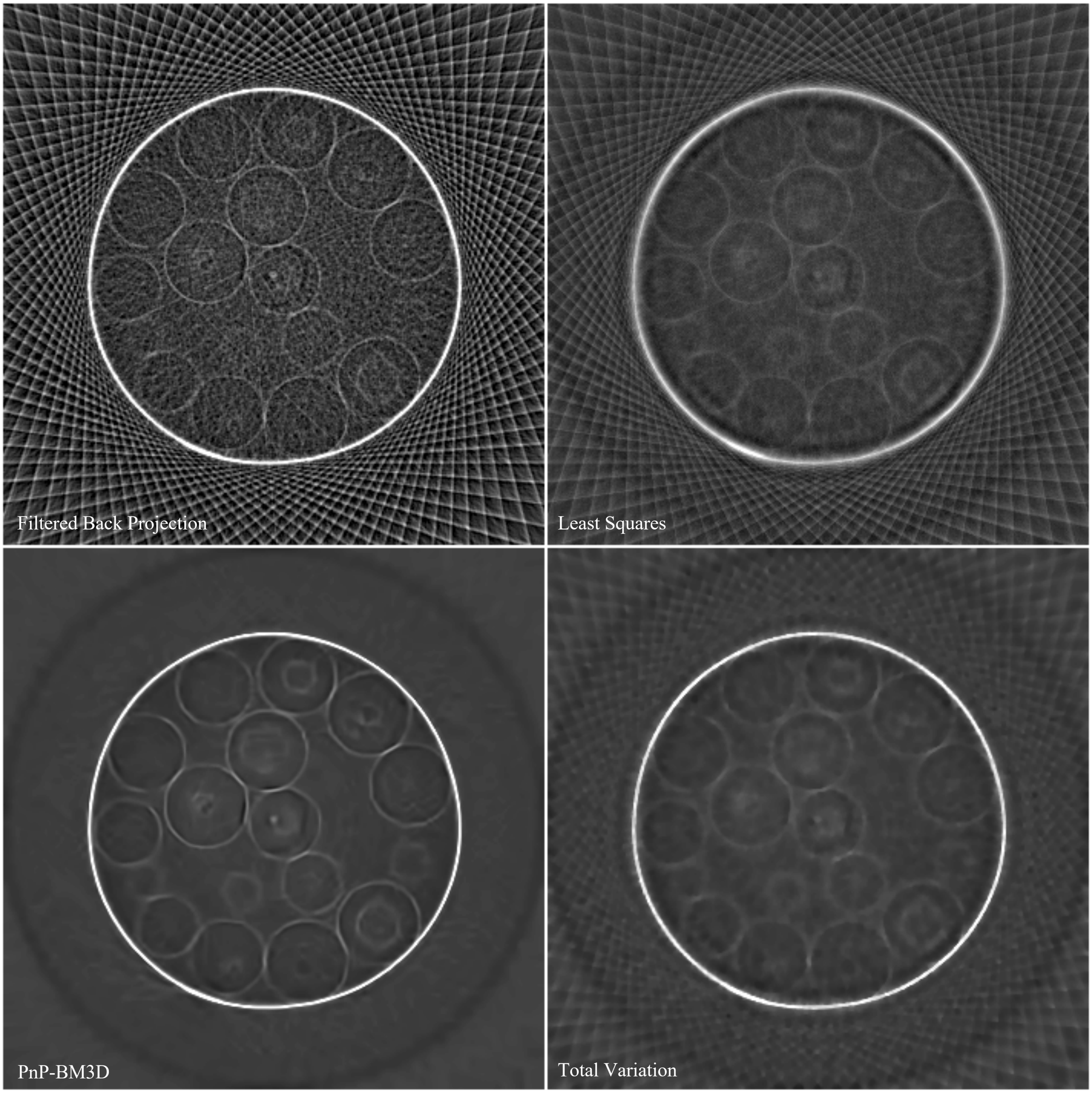

Figure 4: Reconstructions with 90 views. Top left: filtered back projection, top right: unregularized least squares, bottom left BM3D regularized, bottom right total variation regularized. The BM3D reguarlized reconstruction shows superior artifact rejection and contrast.

Due to the lack of ground truth, quantitative assessment is difficult. We treat 450 view BM3D as a pseudo ground truth. Figure 4 shows the pixel values along the middle row of the 450 and 90 view BM3D reconstructions. The 90 view case shows overall good correspondence to real image features in the 450 reconstruction, with some signal loss and reduced ring artifacts.

Figure 5 shows pixel values along the same middle row for the unregularized least squares, BM3D and total variation reconstructions. Notably, the edges of the cup near pixels 75 and 375, circled in the figure, are significantly blurred for both least squares and total variation reconstructions. This is not the case for reconstruction utilizing BM3D, also circled. Comparing Figure 4 and Figure 5, it is clear that the sharp reconstruction at the cup edges is the same in the few and many view cases for BM3D, suggesting that the few view case is adding signal while reducing noise. Other regions along the row show similar behavior.

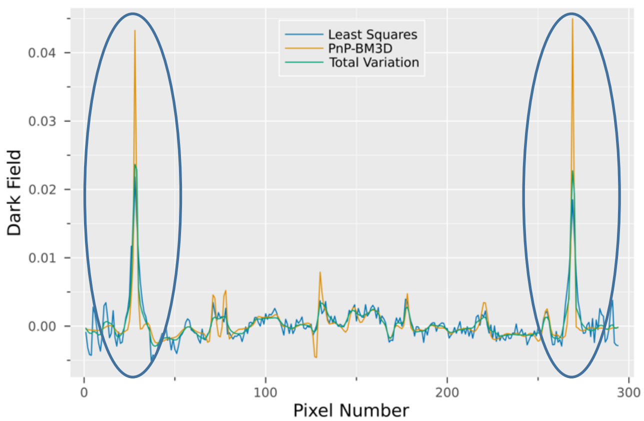

Figure 5: Pixel values along the middle row of the 90 view reconstructions utilizing unregularized least squares, BM3D and total variation as seen in Figure 4. The least squares and total variation cases show a loss of contrast throughout, such as the circled regions corresponding to the edge of the cup.

Conclusion

We demonstrate a sparse view dark field tomographic reconstruction algorithm based on plug-and-play priors and block matching 3D. The resulting algorithm showed improved signal reconstruction with greater noise and artifact suppression than competing traditional techniques like filtered back projection, unregularized least squares, and total variation regularized least squares. This is likely due to an increased capacity for BM3D to retain edge information even in the presence of noise. Data acquisition times present a key obstacle to adoption of XPCI tomography. Our method shows potential for reducing acquisition times by capturing fewer views while retaining essential elements of the reconstructed volume's quality.

References

[1] S. V. Venkatakrishnan, C. A. Bouman, and B. Wohlberg, "Plug-and-play priors for model based reconstruction," in 2013 IEEE Global Conference on Signal and Information Processing, 2013: IEEE, pp. 945-948.

[2] G. T. Buzzard, S. H. Chan, S. Sreehari, and C. A. Bouman, "Plug-and-play unplugged: Optimization-free reconstruction using consensus equilibrium," SIAM Journal on Imaging Sciences, vol. 11, no. 3, pp. 2001-2020, 2018.

[3] D. C.-L. Fong and M. Saunders, "LSMR: An iterative algorithm for sparse least-squares problems," SIAM Journal on Scientific Computing, vol. 33, no. 5, pp. 2950-2971, 2011.

[4] A. Montoison and D. Orban, "Krylov.jl: A Julia Basket of Hand-Picked Krylov Methods," June 2020, doi: 10.5281/zenodo.822073.

[5] K. Dabov, A. Foi, V. Katkovnik, and K. Egiazarian, "Image denoising with block-matching and 3D filtering," in Image processing: algorithms and systems, neural networks, and machine learning, 2006, vol. 6064: SPIE, pp. 354-365.

Author Biography

Johnathan Mulcahy-Stanislawczyk received his BSs in electrical engineering, computer engineering and physics from the Missouri University of Science and Technology (2012) and MSECE from Purdue University (2014). Afterward, he joined the technical staff at Sandia National Laboratories. His interests include computational imaging, computer vision, remote sensing and machine learning.

Amber L. Dagel earned her BA in physics from Middlebury College (2003) and worked in electro-optic infrared active systems at Northrop Grumman before graduate school at the University of Arizona's College of Optical Science to earn her PhD (2011). She has since worked at Sandia National Laboratories with a focus on research in computational imaging across x-ray, remote sensing, synthetic aperture radar, and optical domains.